Reddy, R., Sitz, T. O., Ro-Choi, T. S., & Busch, H. (1974) *Biochem. Biophys. Res. Commun. 56,* 1017–1022.
Ro-Choi, T. S., Moriyama, Y., Choi, Y. C., & Busch, H. (1970) *J. Biol. Chem. 245,* 1970–1977.
Rordorf, B. F., & Kearns, D. R. (1976) *Biochemistry 15,* 3320–3330.
Rubin, G. M. (1973) *J. Biol. Chem. 248,* 3860–3875.
Sanger, F., Brownlee, G. G., & Barrell, B. G. (1965) *J. Mol. Biol. 91,* 235–256.
Sitz, T. O., Kuo, S. C., & Nazar, R. N. (1977) Abstracts of the 174th National Meeting of the American Chemical Society, BIOL 164.
Trapman, J., Delange, P., & Planta, R. J. (1975) *FEBS Lett. 57,* 26–30.
Van, N. T., Nazar, R. N., & Sitz, T. O. (1977) *Biochemistry 16,* 3754–3759.
Weinberg, R. A., & Penman, S. (1968) *J. Mol. Biol. 38,* 289–304.
Yang, S. K., Söll, D. G., & Crothers, D. M. (1972) *Biochemistry 12,* 2311–2320.

Stereodynamics of Dimer Segments of RNA in Aqueous Solution†

M. M. Dhingra,‡ Ramaswamy H. Sarma,* C. Giessner-Prettre, and B. Pullman*

ABSTRACT: Arguments are presented which show that conformations II and III proposed by Lee and Tinoco [Lee, C. H., and Tinoco, I., Jr. (1977), *Biochemistry 16,* 5403] for ribodinucleoside monophosphates in aqueous solution are untenable. It has been shown that ribodinucleoside monophosphates exist in aqueous solution as an equilibrium blend of the classically recognized right-handed stack (g^-g^-), loop stack (g^+g^+), skewed (g^+t), and extended arrays. In order to determine the effect of ϵA base on the conformer distribution in the equilibrium blend, detailed ring-current calculations were performed and the isoshielding curves for ϵA were derived. Use of these curves vis-a-vis dimerization shift data indicates that introduction of ϵA perturbs the equilibrium blend which causes an increase in the population of skewed (g^+t) arrays.

Several theoretical calculations (Perahia et al., 1974; Kim et al., 1973; Govil, 1976) and X-ray diffraction studies (Hingerty et al., 1975; Seeman et al., 1976; Rubin et al., 1972) have shown that ribodinucleoside monophosphates (see Figure 1 for nomenclature) principally display two stacked conformations. In the right-handed stacked conformation, χ_1 and χ_2 are anti, the ribose rings are ^{3}E, ψ_1 and $\psi_2 \simeq 60°$, $\phi_1' \simeq 210°$, $\phi \simeq 180°$, $\omega' \simeq 290°$, and $\omega \simeq 290°$. In the left-handed loop structure the conformational details are same as above, except $\omega' \simeq 80°$ and $\omega \simeq 80°$. NMR studies from this laboratory and that of Danyluk (Lee et al., 1976; Ezra et al., 1977, Cheng and Sarma, 1977a,b; Dhingra and Sarma, 1978a,b) agree with these theoretical projections and solid-state findings. However, recently, Lee and Tinoco (1977) have suggested the existence of three different stacked conformations in aqueous solutions for dinucleoside monophosphates which differ in the magnitude of ω', ω, ϕ', and one of the sugar geometries. Their conformation I is same as the traditional right-handed stack. The conformation II differs from the loop structure in the magnitude of ω' and ω, which are reported to be 30° and 100°, respectively. Conformation III is a new stacked one in which χ_1 is anti, $\chi_2 = 100°$, the sugar of the Np- residue is ^{2}E and that of the -pN residue is ^{3}E, $\phi_1' = 260°$, ψ_1 and $\psi_2 = 60°$, $\phi = 180°$, $\omega' = 50°$, and $\omega = 220°$.

Untenability of Conformation III. In addition to the unusual torsion angles in conformation III, one notices that ^{3}E sugar pucker is coupled to a high value of χ_2 (100°). In view of this, we have been compelled to examine the feasibility of this conformation vis-a-vis the NMR data. From the torsion angles supplied by Lee and Tinoco (1977) and from the known bond lengths and bond angles of nucleic acid structures from X-ray data (Hingerty et al., 1975; Seeman et al., 1976; Rubin et al., 1972), we have derived the atomic coordinates for conformation III. These coordinates were used to construct the perspective of conformation III (Figure 2) using ORTEP II. In developing our arguments, we have used ApA as an example, and it should be emphasized that the nature of the base does not affect the arguments presented. A comparison of Figure 2 with that of conformation III in Figure 7 of Lee and Tinoco (1977) shows important differences. In order to check the validity of their NMR arguments, as well as to check the extent of base parellelism and overlap, we have calculated the cylindrical coordinates z, ρ_6, and ρ_5 for ApA in conformation III. In Table I are given the cylindrical coordinates z, ρ_5, and ρ_6 for the Np residue from the center of the five- and six-membered rings of the -pN residue. In Table II are given the same coordinates for the -pN residue with respect to the Np- residue. Inspection of the magnitude of z for the base carbons, H-2 and H-8 clearly indicates no base parellelism and substantial tilt between the bases. The magnitude of ρ_5 and ρ_6 for base carbons and base protons further reveals no overlap between the bases.

The argument advocated by Lee and Tinoco (1977) for the presence of conformation III is the observation of upfield dimerization shifts for H-5′, H-5″, and H-4′ of the Np- residue by the -pN residue. Inspection of Table I clearly shows that the magnitudes of cylindrical coordinates for H-4′, H-5′ and H-5″

† From the Institute of Biomolecular Stereodynamics and the Department of Chemistry, State University of New York at Albany, Albany, New York 12222, and the Institut de Biologie Physico-Chimique, Paris, France. *Received June 15, 1978.* This research was supported by Grant CA12462 from the National Cancer Institute of the National Institutes of Health and Grant PCM 75-16406 from the National Science Foundation.

‡ Permanent address: Tata Institute of Fundamental Research, Bombay, India.

0006-2960/78/0417-5815$01.00/0 © 1978 American Chemical Society

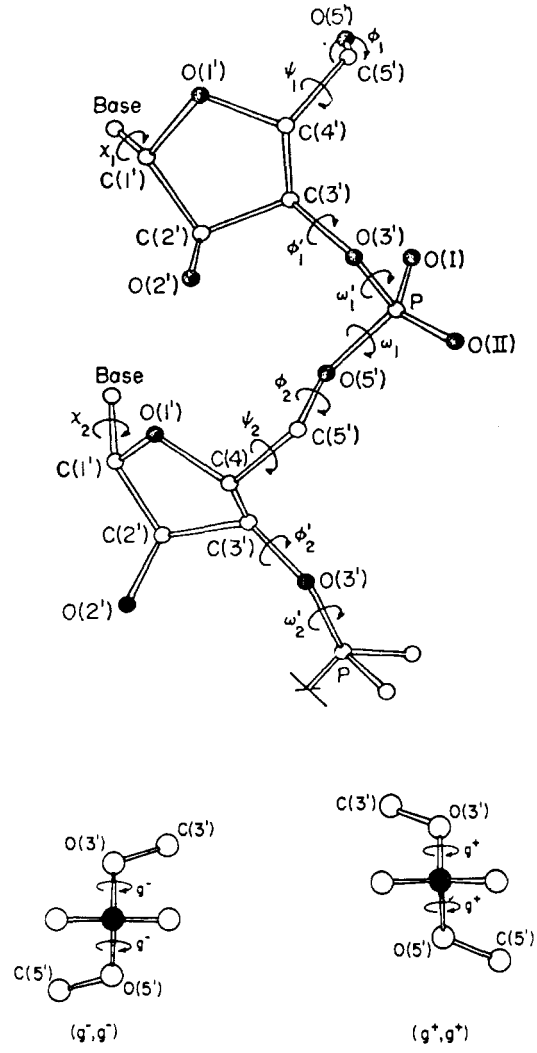

FIGURE 1: Conformational nomenclature.

TABLE I: Cylindrical Coordinates ρ_5, ρ_6, and z in Angstroms for the Various Atoms on the Np- Unit with respect to the -pN Unit in Conformation III.

atoms	z	ρ_5	ρ_6	δ_5^{calcd}	δ_6^{calcd}	$(\delta_5 + \delta_6)^{calcd}$
H-1′	4.4	2.7	2.6	0.10	0.25	0.35
H-2′	5.1	2.4	0.4	0.15	0.37	0.52
H-3′	4.6	1.3	1.9	0.25	0.28	0.53
H-4′[a]	2.3	0.4	2.2	1.58	0.37	1.95
H-5′[a]	1.2	1.7	1.0	0.05	6.89	6.94
H-5″[a]	2.3	2.0	2.2	0.31	0.37	0.68
H-2	6.8	6.6	6.0	0.0	0.0	0.0
H-8	3.1	4.4	2.5	0.0	0.3	0.3
C-2	6.3	6.3	5.4			
C-4	5.0	5.0	3.7			
C-5	4.7	6.1	4.6			
C-6	5.4	7.3	5.8			
C-8	3.7	4.7	3.0			
O-1′	2.8	2.1	1.4	sterically not allowed domains		

[a] Values of z, ρ_5, and ρ_6 for these atoms are sterically not allowed domains.

TABLE II: Cylindrical Coordinates ρ_5, ρ_6, and z in Angstroms for the Various Atoms of the -pN Unit with respect to the Np- Unit in Conformation III.

atoms	z	ρ_5	ρ_6	δ_5^{calcd}	δ_6^{calcd}	$(\delta_5 + \delta_6)^{calcd}$
H-1′	1.5	8.7	10.5	−0.02	−0.02	−0.04
H-2′	2.9	9.3	10.9	−0.02	−0.02	−0.04
H-3′	1.3	9.2	10.4	−0.02	−0.02	−0.04
H-4′	0.8	9.9	11.4	0.0	0.0	0.0
H-5′	2.1	8.3	9.7	−0.02	−0.02	−0.04
H-5″	1.4	9.4	10.6	−0.02	−0.02	−0.04
H-2	1.3	5.7	7.8	−0.06	−0.05	−0.11
H-8	3.0	7.6	9.0	−0.02	−0.02	−0.04
C-2	1.7	5.3	7.4			
C-4	2.1	6.1	7.9			
C-5	2.9	5.1	6.8			
C-6	3.1	3.9	5.9			
C-8	2.9	6.8	8.4			

and O-1′ of Np- are such that they occupy sterically forbidden domains. According to Giessner-Prettre et al. (1976), steric contacts prevent any atom of another group from occupying the region of space $0 \leq |z| \leq 3$ Å, $0 \leq \rho < 4$ Å.

At first, we attempted to remove the bad contacts by using a value of 55° for ω', 215° for ω and 280° for ϕ_1' (vide infra for the experimental value of ϕ_1'). A perspective of this structure is shown in Figure 3b, and the cylindrical coordinates z, ρ_5, and ρ_6 were derived for this conformation. The data showed that several atoms still occupy sterically forbidden domains, rendering this conformation unattainable. The atoms of the Np- residue which occupy sterically forbidden domains along with their cylindrical coordinates are listed on the right-hand side of Figure 3b.

We have further attempted to eliminate bad steric contacts by varying ω' from 40° to 80° and ω from 190° to 230°. In this conformational search, the experimentally determined value of $\phi_1' = 277$ (Lee and Tinoco, 1977) was used, and the rest of the torsion angles were maintained to those proposed by Lee and Tinoco (1977). In the conformation space searched, we were unable to locate a domain in which all the bad contacts were eliminated. Perspectives of some of these conformations are shown in Figure 3a,c,d. Also given are the cylindrical coordinates for atoms of the Np- residue in sterically forbidden domains. In addition, we have attempted to generate sterically allowed conformations using the best obtained $\omega'\omega$ combinations by decreasing the unusually high value of χ_2 (100°) employed by Lee and Tinoco for a ^{3}E sugar pucker. The value of χ_2 was at first decreased to 80° and then to 50°, and this did not remove bad contacts (Figure 4a,b)

Based on the above, as well as on the plethora of theoretical, X-ray, and NMR work cited at the beginning, one has to conclude that conformation III proposed by Lee and Tinoco (1977), as well as those in the ranges of ω' 40°–80°, ω 190–230° while maintaining Lee–Tinoco torsion angles for the backbone, is not allowed for dinucleoside monophosphates.

Untenability of Conformation II. From the given torsion angles in Lee and Tinoco (1977) and X-ray data on nucleic acid structure, we have derived the atomic coordinates for conformation II, and the ORTEP II projection of it is shown in Figure 5. The cylindrical coordinates are given in Tables III and IV. The data indicate sterically nonallowed domains for certain atoms, but they are just at the border of being nonallowed and, hence, can be approximated to allowed domains and ring-current effects can be computed. The problem with conformation II is that the arguments presented by Lee and Tinoco (1977) for the existence of this conformation, viz., the upfield shifts of the H-2′ of -pN and the H-3′ of Np- residues, are wrong. The data in Table III indicate that H-2′ of the -pN residue will be shielded, as has been indicated by Lee and Tinoco (1977). The authors indicate that H-3′ of Np- in conformation II will be *shielded,* but the data in Table IV show that the coordinates for H-3′ of Np- are such that this proton

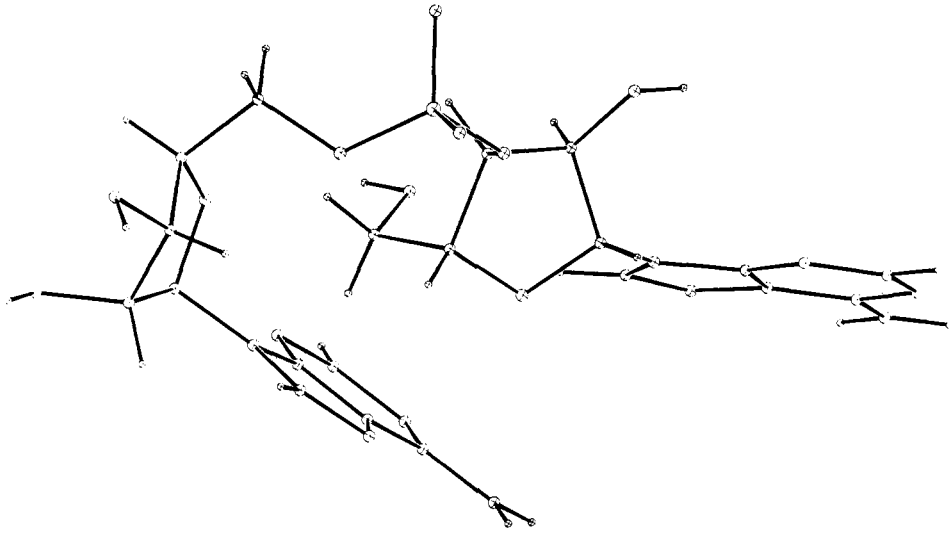

FIGURE 2: ORTEP II projection of conformation III of Lee and Tinoco (1977). The ribose of Np is ^2E and that of -pN is ^3E. The remaining torsion angles are: $\chi_1 = 40°$, $\phi_1' = 260°$, $\omega' = 50°$, $\omega = 220°$, $\phi_2 = 180°$, $\psi_2 = 60°$, $\chi_2 = 100°$, and $\psi_1 = 60°$. In the computer output there was a covalent bond between the H-5′ of Np- and the C-4 of the adenine of -pN. A bond was drawn by the program because the distance between the above atoms was less than 1.67 Å. This bond has been removed from the above figure for clarity.

TABLE III: Cylindrical Coordinates ρ_5, ρ_6, and z in Angstroms for the Various Atoms of the -pN Unit with respect to the Np- Unit in Conformation II.

atoms	z	ρ_5	ρ_6	δ_5^{calcd}	δ_6^{calcd}	$(\delta_5 + \delta_6)^{calcd}$
H-1′	5.4	3.0	4.5	0.00	0.00	0.00
H-2′[a]	2.8	2.7	4.4	0.16	0.10	0.26
H-3′[a]	2.8	2.8	4.9	0.09	0.10	0.19
H-4′	5.0	4.6	6.6	0.00	0.00	0.00
H-5′	5.7	4.4	6.4	0.00	0.00	0.00
H-5″	4.1	4.9	6.9	0.00	0.00	0.00
H-2	5.4	5.0	4.4	0.00	0.00	0.00
H-8	4.1	1.2	3.1	0.25	0.12	0.37
C-2	5.1	4.0	3.3			
C-4	4.7	1.8	2.1			
C-5	4.4	1.9	0.9			
C-6	4.5	3.3	1.6			
C-8	4.2	0.3	2.2			

[a] Values of z, ρ_5, and ρ_6 for these atoms represent sterically not allowed domains.

TABLE IV: Cylindrical Coordinates ρ_5, ρ_6, and z in Angstroms for the Various Atoms of the Np- Unit with respect to the -pN Unit in Conformation II.

atoms	z	ρ_5	ρ_6	δ_5^{calcd}	δ_6^{calcd}	$(\delta_5 + \delta_6)^{calcd}$
H-1′	3.9	4.9	6.7	0.00	0.00	0.00
H-2′	1.5	3.8	5.7	−0.10	−0.10	−0.20
H-3′	1.6	4.3	6.4	0.00[a]	−0.08	−0.08
H-4′	2.9	6.7	8.8	0.00	−0.02	−0.02
H-5′	3.9	6.6	8.7	0.00	0.00	0.00
H-5″	2.2	6.6	8.6	−0.03	−0.03	−0.06
H-2	3.6	4.7	5.0	0.00	0.00	0.00
H-8	4.2	3.1	5.1	0.00	0.00	0.00
C-2	3.8	3.6	4.1			
C-4	3.9	2.4	4.0			
C-5	4.3	1.2	2.8			
C-6	4.4	1.7	2.0			
C-8	4.2	2.3	4.4			

[a] This atoms lies right at a zone in which shielding and deshielding zones are changing. No data for this are given by Giessner-Prettre et al. (1976). However, it is obvious that this atom will experience either negligible effect or a slight deshielding.

will experience *deshielding*. For the above reasons, conformation II is untenable.

Since conformations II and III are untenable, the observed shift trends for the H-3′, H-4′, H-5′, and H-5″ of the Np- residue and that for the H-2′ of the -pN residue should be rationalized. We have indicated elsewhere (Lee et al., 1976; Ezra et al., 1977; Sarma and Danyluk, 1977; Dhingra and Sarma, 1978b) that these shift trends, as well as a large number of other shift trends, are easily rationalized on the basis of a conformational blend of right-handed stack (g^-g^-, i.e., P_3, Kim et al., 1973), loop stack (g^+g^+, i.e., A_1, Kim et al., 1973), and skewed and extended arrays (e.g., g^+t, i.e., S_1, tg^+, i.e., A_2, Kim et al., 1973). We address below only those shifts attributed to conformations II and III.

Upfield Shift of H-5′ and H-5″ of the Np- Residue in PUPU and PYPU Dimers. The upfield shifts of H-5′ and H-5″ of the Np- residue range from 0.440 to 0.009 ppm for H-5′ and from 0.238 to 0.024 for H-5″ (Table V). These shifts cannot originate from g^-g^- conformers because the protons are far removed from the -pN residue. Examination of the seven possible conformations for ribodinucleoside monophosphates

TABLE V: Dimerization Data in Parts per Million at 20 °C for the H-3′, H-4′, H-5′, and H-5″ of the Np- Residue for Dimers Taken from the Microfilm Supplied by Lee and Tinoco (1977).[a]

dimer	residue	H-3′	H-4′	H-5′	H-5″
ϵApϵA	ϵAp-	0.159	0.203	0.192	0.131
ApϵA	Ap-	0.166	0.264	0.309	0.166
ApA	Ap-	0.110	0.097	0.009	0.024
ϵApG	ϵAp-	0.165	0.228	0.202	0.200
ApG	Ap-	0.111	0.116	0.069	0.058
GpϵA	Gp-	0.177	0.276	0.341	0.218
GpA	Gp-	0.098	0.114	0.056	0.081
UpϵA	Up-	0.122	0.252	0.440	0.238
UpA	Up-	0.085	0.086	0.133	0.121
ϵApU	ϵAp-	0.130	0.000	−0.075	−0.003
ApU	Ap-	0.123	−0.006	−0.103	0.034
CpC	Cp-	0.106	−0.030	−0.057	−0.007

[a] We have been informed by Dr. Lee that some of the data in the microfilm were wrong and he has supplied us the corrected data. These corrected data were employed in Table V.

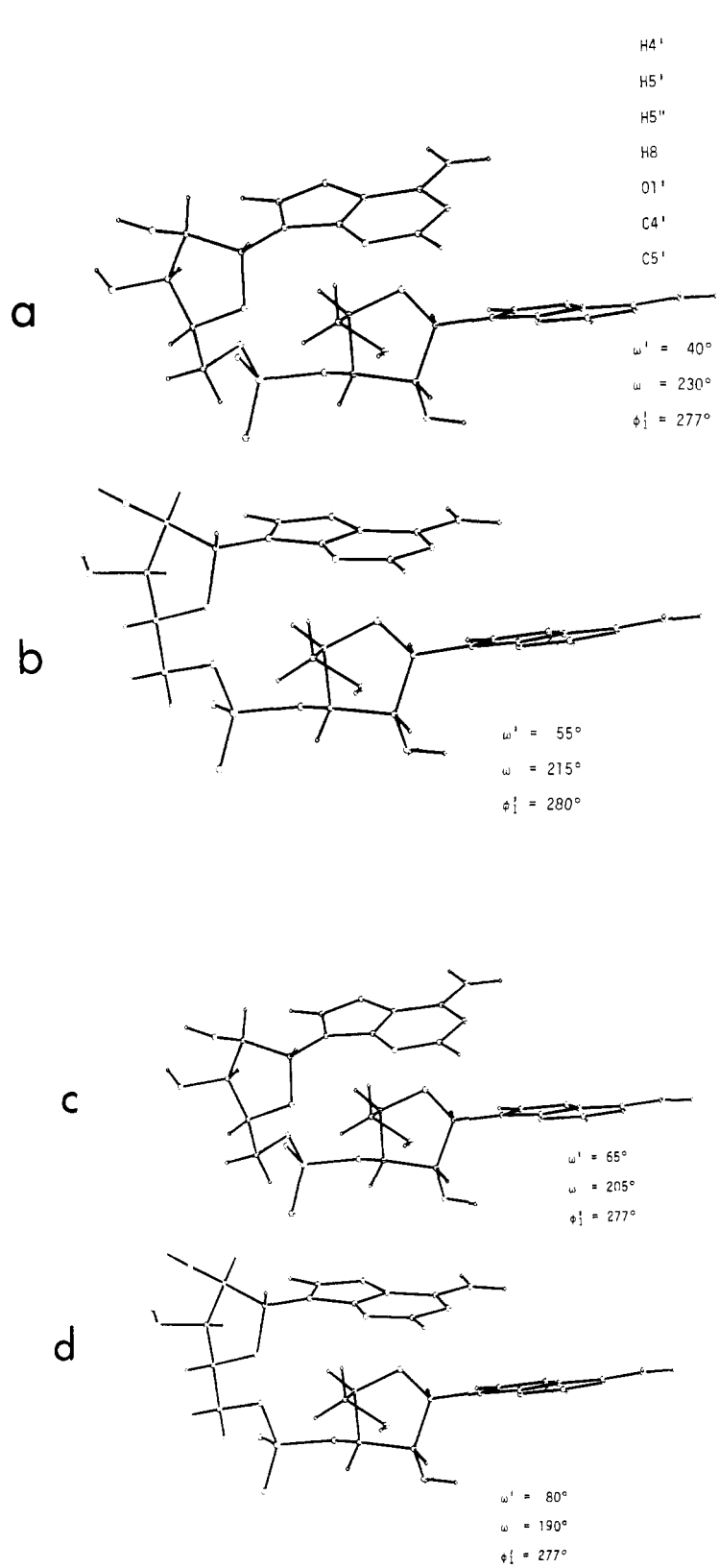

	z	ρ_5	ρ_6
H4'	2.4	0.3	2.4
H5'	1.2	1.9	1.8
H5"	2.5	2.4	2.9
H8	2.5	4.3	2.2
O1'	2.6	1.7	0.9
C4'	2.8	0.6	1.5
C5'	2.2	1.9	1.9

	z	ρ_5	ρ_6
H4'	2.3	0.5	2.5
H5'	1.6	2.2	1.8
H5"	3.1	2.4	2.5
H8	2.3	4.1	2.2
C8	2.5	4.4	2.7
O1'	2.2	1.5	1.3
C4'	2.8	0.6	1.6
C5'	2.6	2.0	1.7

	z	ρ_5	ρ_6
H4'	2.3	0.4	2.4
H5'	1.8	2.1	1.4
H5"	3.3	2.2	2.1
H8	2.4	4.2	2.5
C8	2.5	4.5	3.1
O1'	2.2	1.6	1.6
C4'	2.8	0.5	1.6
C5'	2.8	1.9	1.2

	z	ρ_5	ρ_6
H4'	2.4	0.3	2.3
H5'	2.2	2.1	0.7
H8	2.4	4.3	3.1
O1'	2.2	1.8	2.1

FIGURE 3: (a,b) These figures illustrate the effect of changing ω', ω, and ϕ_1' on conformation III. In a, $\omega' = 40°$, $\omega = 230°$, and $\phi_1' = 277°$. In b, $\omega' = 55°$, $\omega = 215°$, and $\phi_1' = 280°$. On the right-hand side of the figures are given the cylindrical coordinates z, ρ_5 and ρ_6 for atoms of the Np- unit which occupy sterically forbidden domains. (c,d) These figures again illustrate the effect of changing ω, ω', and ϕ_1' as in Figure 3a. In c, $\omega' = 65°$ and $\omega = 205°$. In d, $\omega' = 80°$ and $\omega = 190°$. The data on the right-hand side are the coordinates of the atoms which occupy sterically forbidden domains in the Np- unit.

(Kim et al., 1973) suggests that g^+g^+ (A_1), g^+t (S_1), and tg^+ (A_2) conformations (Figure 6a,b,c) may account for the shielding of these protons. We have derived the cylindrical coordinates and the projected shieldings for these protons in these conformations, and these are given in Table VI. The data clearly indicate that in the g^+t conformation H-5′ and H-5″ protons of the Np- residue will experience substantial shielding from the ring-current field of the base at the -pN residue

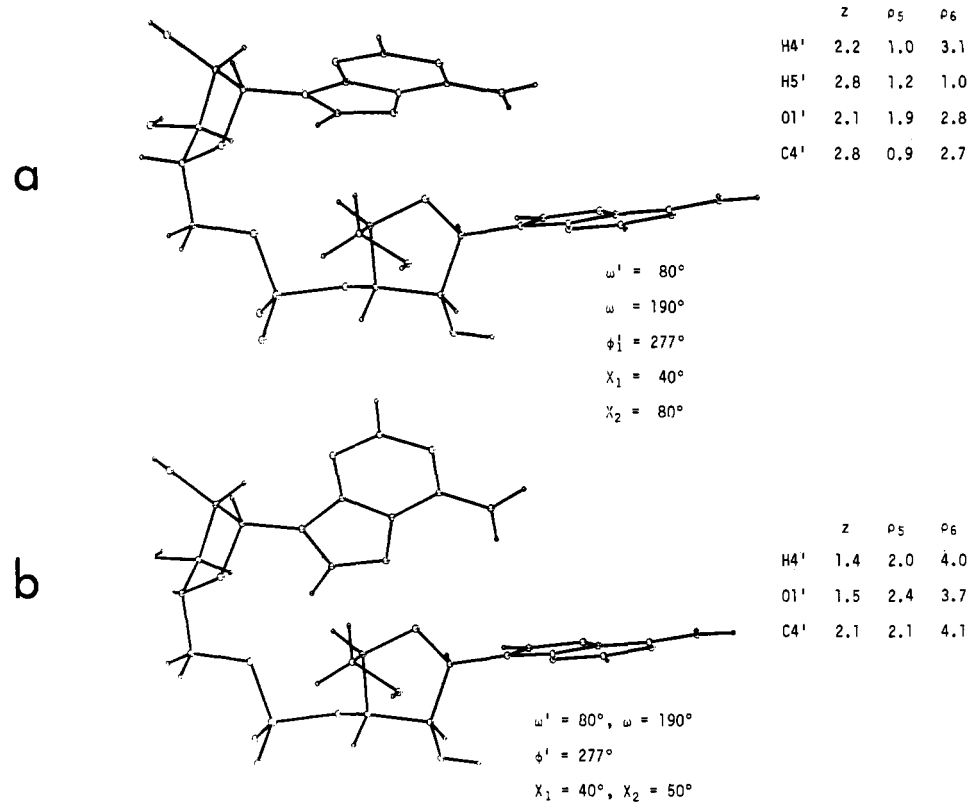

FIGURE 4: Effect of changing χ_2 on the conformation in Figure 3d. In a, $\chi_2 = 80°$; in b, $\chi_2 = 50°$. Again, data on the right-hand side provide the coordinates of atoms residing in sterically forbidden domains in the Np- unit.

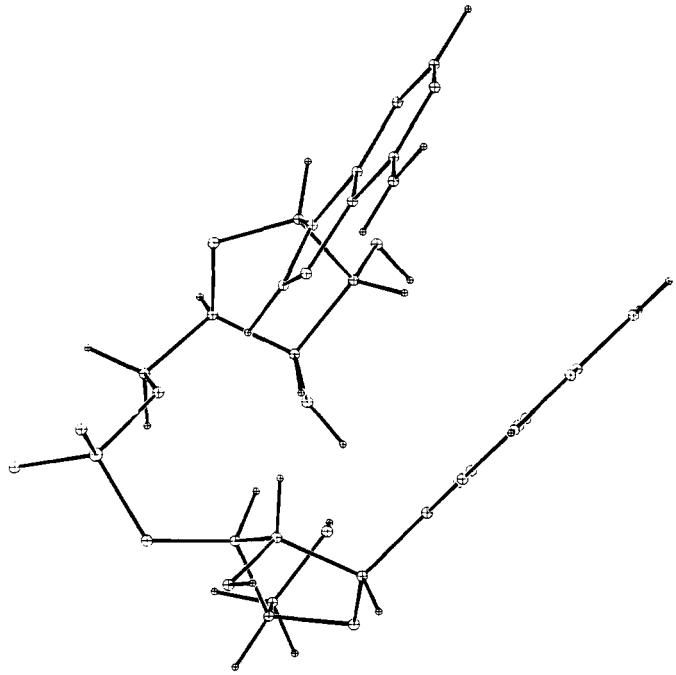

FIGURE 5: An ORTEP II projection of conformation II of Lee and Tinoco (1977). The riboses of both nucleotidyl units are ^3E. The remaining torsion angles are: $\chi_1 = 20°$, $\phi_1' = 205°$, $\omega' = 30°$, $\omega = 100°$, $\phi_2 = 180°$, $\psi_2 = 60°$, $\chi_2 = 40°$, and $\chi_1 = 60°$.

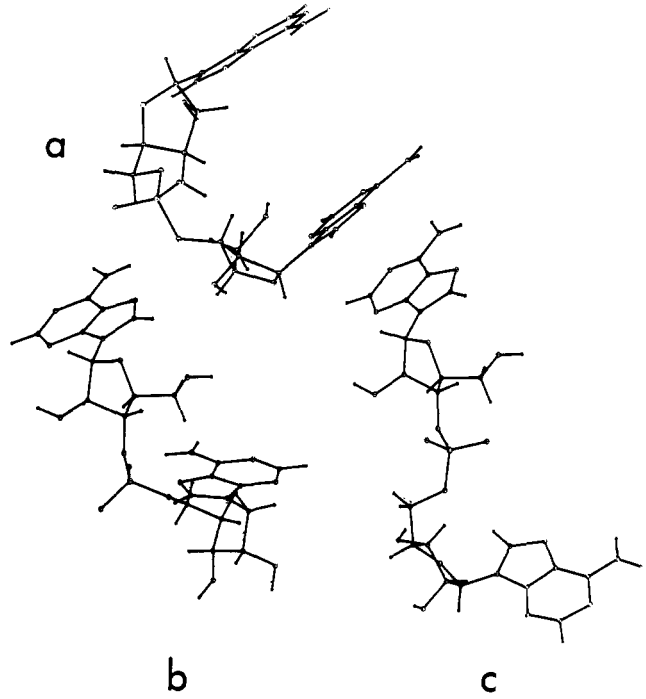

FIGURE 6: ORTEP II projections of (a) g^+g^+ ($\omega' = 80°$, $\omega = 80°$, A_1), (b) g^+t ($\omega' = 110°$, $\omega = 215°$, S_1), and (c) tg^+ ($\omega' = 180°$, $\omega = 80°$, A_2) conformations. In all projections the riboses of both units are ^3E and torsions about χ, ψ, ϕ' and occupy classical domains.

(Figure 6b). The data in Table VI further reveal that contribution to the shielding of H-5′ and H-5″ of Np- from the tg^+ conformation is negligible and that from g^+g^+ is relatively small. Hence, the observed shielding of H-5′ and H-5″ of the Np- residue in PUPU and PYPU dimers can be reasonably interpreted to originate from a mixture of g^+g^+, g^+t, and tg^+ arrays in which g^+t predominates; otherwise, one has to invoke the unreasonable assumptions such as nearly 100% g^+g^+ conformer plus minor contributions from the skewed g^+t arrays. The calculations in Table VI have been performed employing Remin-Shugar (1972) assignments for H-5′ and

TABLE VI: Cylindrical Coordinates z, ρ_5, and ρ_6 in Angstroms and Projected Shielding in Parts per Million for H-5′ and H-5″ of the Np- Residue in Various Conformations.

conformation	proton	cylindrical coordinates			projected shielding		
		z	ρ_5	ρ_6	δ_5	δ_6	$\delta_5 + \delta_6$
g^+g^+ ($\omega' = 80°$; $\omega = 80°$)	H-5′	6.5	3.0	4.8	0.10	0.00	0.10
	H-5″	5.0	3.5	5.3	0.08	0.00	0.08
g^+t ($\omega' = 110°$; $\omega = 215°$)	H-5′	4.1	1.2	2.8	0.27	0.22	0.49
	H-5″	3.1	1.5	3.5	0.38	0.06	0.44
tg^+ ($\omega' = 180°$; $\omega = 80°$)	H-5′	7.3	3.8	5.7	0.03	0.00	0.03
	H-5″	5.7	3.4	5.4	0.05	0.00	0.05
g^-g^- ($\omega' = 285°$; $\omega = 295°$)	H-5′	5.9	5.0	6.9	0.00	0.00	0.00
	H-5″	4.4	5.5	7.5	0.00	0.00	0.00

TABLE VII: Internuclear Distance r in Angstroms between the H-5′ and H-5″ of the Np- Residue and the 2′-OH and 3′-OH of the -pN Residue and Phosphodiester Oxygens in Various Conformations.

conformation	proton	2′-OH	3-′OH	phosphate (O)	phosphate (O)
g^+g^+ ($\omega' = 80°$; $\omega = 80°$)	H-5′	6.4	3.9[a]	6.2	5.9
	H-5″	5.4	2.9[a]	4.8	4.7
g^+t ($\omega = 110°$; $\omega = 215°$)	H-5′	7.8	8.0	6.3	5.4
	H-5″	6.4	6.4	5.0	4.1[a]
tg^+ ($\omega' = 180°$; $\omega = 80°$)	H-5′	9.5	7.4	5.0	6.1
	H-5″	8.3	6.4	3.5[a]	4.9
g^-g^- ($\omega' = 285°$; $\omega = 295°$)	H-5′	10.9	9.9	5.1	5.8
	H-5″	10.0	8.7	3.6	4.3

[a] Distances are close enough to H-5′ and H-5″ of Np- to cause deshielding.

H-5″. The data indicate that H-5′ is shielded more than H-5″

In fact, Lee and Tinoco (1977) argue that H-5′ is more sensitive to dimerization than H-5″ and present this as evidence for conformation III which we have shown to be untenable. Examination of the data in Table V indicates that, in all cases, H-5′ is not shielded more than H-5″. For example, in ApA and GpA, it is the H-5″ which undergoes larger shielding; in ϵApG, both H-5′ and H-5″ are shielded to the same extent. This nonuniformity exists in the shielding pattern of H-5′ and H-5″ of the Np- of the various dimers because they are highly sensitive to small variations in ω', ω, and χ_2. For example, in the g^+t conformation shown (Figure 6b), $\omega' = 110°$, $\omega = 215°$, and $\chi_2 = 50°$, and this results in the shielding of H-5′ shown in Table VI. If $\omega' = 115°$, $\omega = 200°$, and $\chi_2 = 70°$, the H-5″ will be shielded to a considerably larger extent than H-5′. In addition, the observed magnitude and direction of the shifts of H-5′ and H-5″ of Np- can be affected from the shielding/deshielding originating from the 3′-OH of the -pN residue and the phosphate oxygens, and this is discussed in the next section.

Downfield Shifts of H-5′ and H-5″ of the Np- Residue in PYPY and PUPY Dimers. When a pyrimidine occupies the -pN residue, one always detects a small, but real, downfield shift of H-5′ and H-5″ of the Np- residue (Table V). These downfield shifts originate from, again, a blend of g^+g^+, tg^+, and g^+t conformations. Because the pyrimidine at the -pN part has very little shielding effect (Giessner-Prettre et al., 1976), the deshielding exerted by the 3′-OH of the -pN residue as well as the phosphate oxygens becomes apparently dominant and manifests as deshielding effects (see Table VII for distances). In PUPU and PYPU dimers, even though these deshielding effects are present, they are masked by the strong shielding effect of the purine at -pN. A dramatic example of these countereffects is provided by the data for H-5′ and H-5″ of the Np- residue in ϵApU and UpϵA (Table V).

Upfield Shifts of H-3′ of the Np- Residue in All Dimers. Inspection of Table V reveals that in all dimers, irrespective of the nature of the base at the Np- and -pN parts, the H-3′ of the Np- residue has undergone shielding upon dimerization. In those dimers in which -pN is a purine, one can attribute part of the shifts to ring-current effects from an adjacent residue in g^-g^- and g^+g^+ conformers. However, the very important observation is that these upfield shifts of H-3′ of Np- are generally independent of whether -pN is a purine or a pyrimidine and, hence, a sizable contribution should originate from nonbase sources. This peculiar behavior of H-3′ of Np- was first observed by Cheng and Sarma (1977a,b), who showed that the shielding of H-3′ is associated with the transformation of a relatively freely rotating O-3′–P bond in the 3′-mononucleotide to a phosphodiester linkage in the dimer. Dimerization and formation of the phosphodiester linkage would introduce some constraint about O-3′–P torsion, and flexibility becomes limited to certain domains. It was specifically pointed out (Cheng and Sarma, 1977a,b) that transformation of a freely rotating O-3′–P bond in the monomer to the g^- domain in the dimer ($\omega' = g^-$ as in g^-g^- conformation) will cause shielding of H-3′ of Np-. The observed upfield shifts of H-3′ of Np- (Table V), *irrespective of the nature of the base* on either ends, indicate that upon dimerization the O-3′–P (ω') bond of the dimer occupies g^- domains as, for example, in a g^-g^- conformation. Obviously, the magnitude of the shift will be determined by the occupied local domain in the g^- conformation space about ω' as well as by the percentage population of such conformers.

Upfield Shifts of the H-4′ of the Np- Residue. The data in Table V indicate that in PUPU and PYPY dimers the H-4′ of the Np- residue undergoes significant shielding. On the other

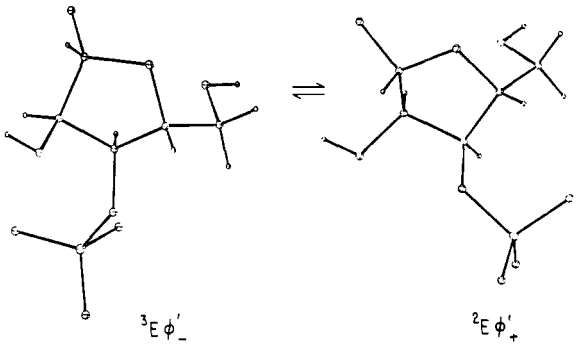

FIGURE 7: This figure illustrates the position of the phosphate group with respect to H-4′ in $^3E\phi_-'$ and $^2E\phi_+'$ conformations.

hand, in PUPY and PYPY dimers, this proton shows no significant dimerization shifts. The major effect on δ H-4′ upon dimerization originates from a shift of $^2E\phi_+' \rightleftharpoons {}^3E\phi_-'$ equilibrium. It is known that purine 3′-mononucleotides predominantly exist in the $^2E\phi_+'$ (60–65%; data from Lee and Tinoco, 1977) conformation, but upon dimerization the population of $^3E\phi_-'$ becomes predominant (60–70%; data from Lee and Tinoco, 1977) in PUPY and PUPU dimers. Inspection of the perspectives in Figure 7 clearly reveals that a shift from the $^2E\phi_+'$ to the $^3E\phi_-'$ conformation removes the deshielding phosphate group from the vicinity of H-4′ of Np-, and this causes the H-4′ shift to higher fields. The variation of the theoretically calculated chemical shift of the protons of the ribose of 3′-AMP as a function of ϕ' (Giessner-Prettre and Pullman, 1978) (Figure 8a,b) clearly demonstrates the sensitivity of the H-4′ chemical shift to the magnitude of ϕ'. Interestingly, pyrimidine 3′-mononucleotides display 40–45% (data from Lee and Tinoco, 1977) preference for $^2E\phi_+'$, i.e., the pyrimidine 3′-mononucleotides have, to begin with, on the average about 55–60% the population of the $^3E\phi_-'$ conformation, and upon dimerization in PYPU and PYPY dimers no substantial shifts of $^2E\phi_+' \rightarrow {}^3E\phi_-'$ take place. The average population of $^3E\phi_-'$ conformers in PYPU and PYPY dimers is about 65% (data from Lee and Tinoco, 1977). This explains the lack of any significant shielding of the H-4′ of the Np-residue in PYPU and PUPU dimers.

Shift Trends of H-2′ of the -pN Residue upon Dimerization. Data in Lee and Tinoco (1977, microfilm) indicate that in the collection of molecules examined the H-2′ of -pN undergoes dimerization shifts in the range of +0.355 ppm in ApA to −0.030 ppm in UpεA. In GpεA, the effect is negligible (0.002 ppm). Primarily two factors can affect the shift of H-2′ upon dimerization. (1) Dimerization and formation of a g^-g^- stacked array in PUPY and PUPU dimers can cause an upfield shift of H-2′ of -pN. This originates from the ring-current effect of the purine at Np-. For example in ApA, this effect could be as much as 0.13 ppm (Dhingra and Sarma, 1978a). Inspection of the data in Lee and Tinoco (1977, microfilm) shows that the H-2′ of -pN in GpεA has undergone no shift; in UpA and CpC, the shifts are to the high field by 0.147 and 0.132 ppm, respectively; but in UpεA it has undergone a slight shift to low field. Obviously, a second factor other than ring currents of the Np- residue influences H-2′ of -pN. (2) This factor has to do with the change in χ_2 upon dimerization. One cannot realistically project the direction and magnitude of the shift of δ H-2′ of -pN due to change in χ without the knowledge of actual χ values in the monomer and dimer. NMR data indicate that for both dimers and monomers χ_2 is in the *anti domain* and that χ_2 undergoes reduction upon dimerization, but actual magnitudes are unknown, and this creates serious problems

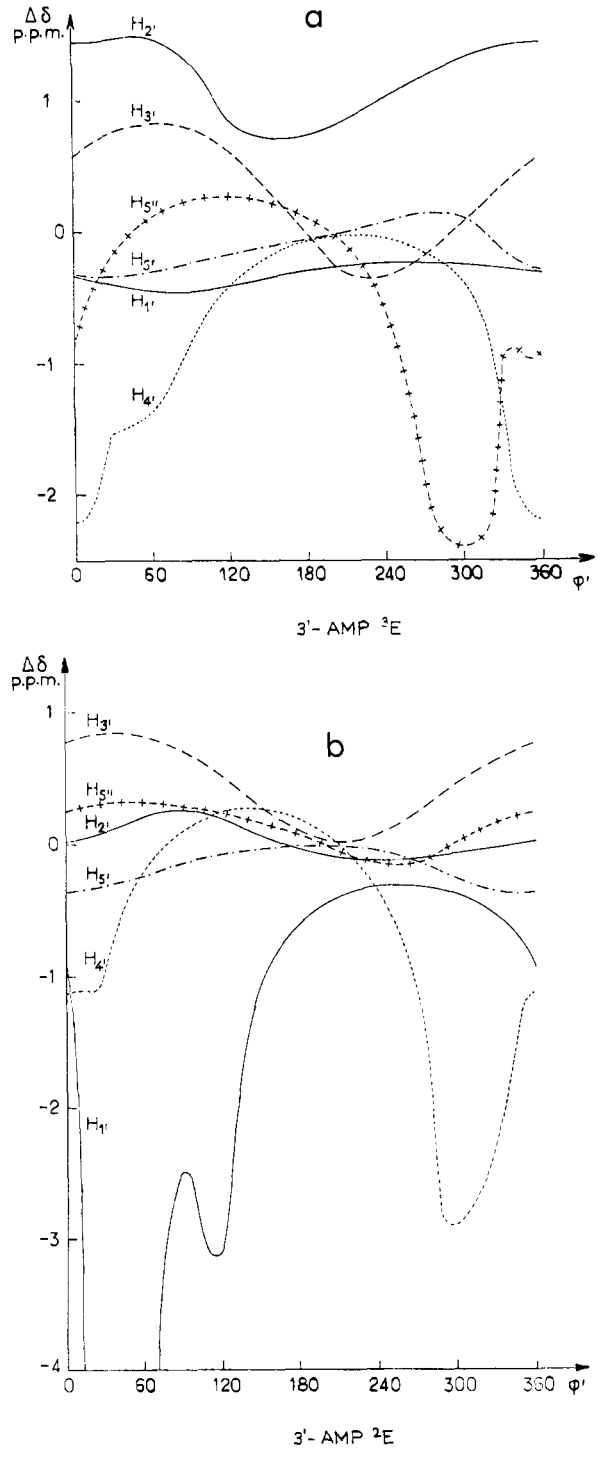

FIGURE 8: Variation of the chemical shift of ribose protons against ϕ' in 3′AMP: (a) ^3E; (b) ^2E. The ϕ' follows the notation of Sundaralingam.

to clearly explain the shift trends of H-2′ of -pN. A few examples are illustrated below under conditions in which sugar pucker is ^3E: (a) suppose that the value of χ in 5′-AMP is 70° and upon formation of ApA χ_2 becomes 40° and this will cause shielding of H-2′; (b) on the other hand, a substantial change from 60° to 20° will have no effect on H-2′; (c) but a change from 40° to 20° will cause deshielding. This information is taken from Giessner-Prettre and Pullman (1977). From the above discussion it is obvious that one cannot use the dimerization data on H-2′ alone effectively to obtain information about the spatial configuration of oligonucleotides.

Conformational Properties of εApεA and Other Dimers

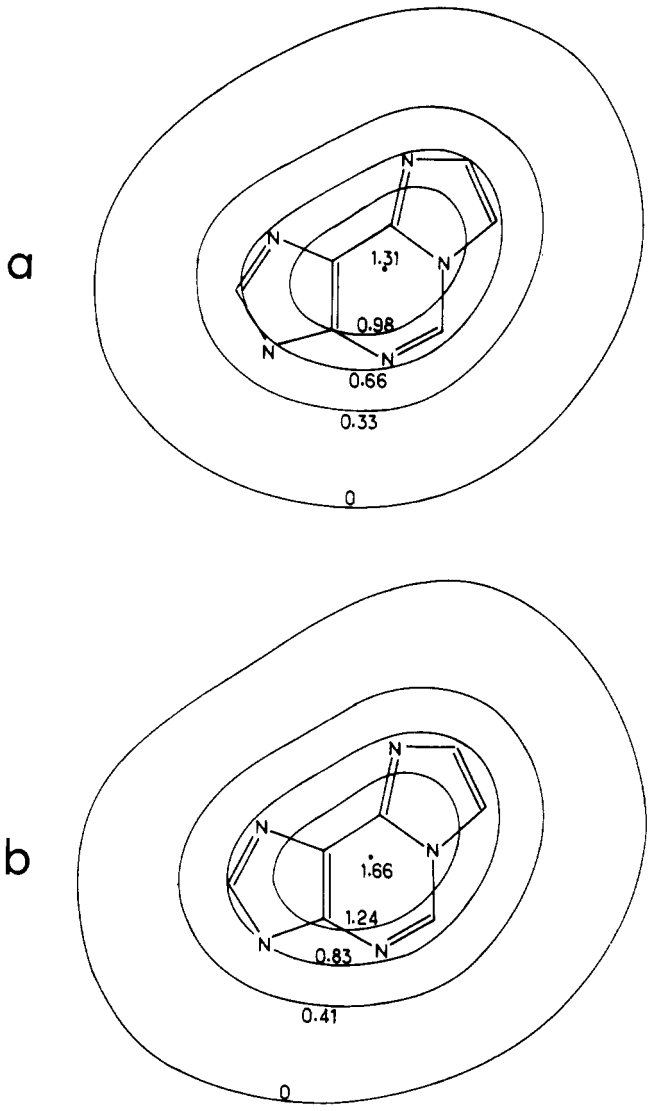

FIGURE 9: (a) Intermolecular shielding ($\Delta\delta$) due to the ring current in ϵA (in a plane 3.4-Å distant from the molecular surface). (b) Intermolecular shielding values ($\Delta\delta$) due to the sum of the ring-current effect and of the atomic diamagnetic susceptibility anisotropy in ϵA (in a plane 3.4-Å distant from the molecular surface).

Containing ϵA. It has been shown above, using ApA as an example, that the dimerization shifts of various protons for both the nucleotidyl units of the dimers can be accounted for by the presence of an equilibrium blend of g^-g^-, g^+g^+, g^+t, and tg^+ conformers in aqueous solution. A comparison of the dimerization data of ϵA-containing dimers with that of the parent dinucleoside monophosphates shows that the dimerization has substantially large effects in many of the ϵA-containing systems, particularly for the base protons of the Np- residue and H-5′ and H-5″ protons of the -pN residue (Tables V and VII). For example, in ϵApϵA, the H-2 and H-8 of pϵA undergo a dimerization shift of 0.34 to 0.32 ppm, whereas the corresponding shifts in ApA range from 0.11 to 0.24 ppm (Table VIII). In UpϵA, the H-5′ and H-5″ of Up- are shielded by as much as 0.44 and 0.24 ppm, respectively, whereas the corresponding shifts in UpA are only 0.13 and 0.12 ppm (Table V). These differences in dimerization data between the parent and ϵA containing dimers may arise from the following situations alone or in combinations: (1) The ring-current fields of ϵA are significantly different from that of A. (2) The conformational equilibrium among the various proposed stacked and extended arrays is perturbed by the introduction of ϵA. (3)

TABLE VIII: Dimerization Data in Parts per Million at 20 °C for H-5′, H-5″ and the Base Protons of the -pN Residue for Dimers taken from the Microfilm Supplied by Lee and Tinoco (1977).

dimer	residue	H-5′	H-5″	H-2- (H-5)	H-8- (H-6)	H-10	H-11
ϵApϵA	−pϵA	−0.249	−0.112	0.338	0.324	0.228	0.231
ApϵA	−pϵA	−0.186	−0.052	0.082	0.222	0.225	0.255
ApA	−pA	−0.246	−0.048	0.114	0.244		
ϵApG	−pG	−0.220	−0.105		0.301		
ApG	−pG	−0.220	−0.086		0.208		
GpϵA	−pϵA	−0.178	−0.083	0.083	0.208	0.222	0.219
GpA	−pA	−0.217	−0.057	0.084	0.170		
UpϵA	−pϵA	−0.158	−0.103	−0.058	0.102	0.014	0.041
UpA	−pA	−0.122	−0.026	0.020	0.065		
ϵApU	−pU	−0.218	−0.075	0.388	0.280		
ApU	−pU	−0.199	−0.055	0.374	0.263		

Introduction of ϵA causes significant changes in certain key torsion angles and overall molecular topology.

In order to help us to distinguish among the above possibilities, we have calculated the isoshielding curves for ϵA using methodology described earlier (Giessner-Prettre and Pullman, 1970; Johnson and Bovey, 1958; Waugh and Fessenden, 1957; Giessner-Prettre and Pullman, 1965, 1969; Giessner-Prettre et al., 1976). The results are expressed as a set of isoshielding contours in parts per million for the ϵA base at a z value of 3.4 Å. This is shown in Figure 9a. In addition, we have also calculated the shielding contours due to the sum of the ring-current effect and the atomic diamagnetic susceptibility anisotropy in ϵA in a plane 3.4-Å distant from the molecular surface. This is shown in Figure 9b. In order to simplify the use of ring-current surfaces, the shielding from each of the three rings of ϵA is presented in a series of graphs in which the value of $|z|$ (vertical distances from the base planes) ranges from 0 to 8 Å and ρ (the radial distances from the center of the ring) from 0 to 10 Å (Figure 10a-c). This type of representation has already been published for the normal nucleic acid bases (Giessner-Prettre et al., 1976).

A comparison of the isoshielding curves for ϵA and A (Giessner-Prettre et al., 1976) shows that the addition of an extra five-membered ring (N-1-N-6) in ϵA significantly alters the ring-current effects of the six-membered ring. For example, in A, the maximum shielding of 1.40 ppm is projected for the six-membered ring when $\rho = 0$ and $z = 3.0$ Å. In ϵA the corresponding number is 1.05 ppm. On the other hand, for the five-membered ring (N-7-N-9) of ϵA, there is a slight increase in the overall shielding effect.

It has been shown elsewhere (Lee et al., 1976; Ezra et al., 1977) that the dimerization data on H-5′ of the -pN residue is a clear monitor of the presence of g^-g^- phosphodiester torsions in ribodinucleoside monophosphates. This has been explained as due to the deshielding effect of the 2′-OH of the Np- residue. In the g^-g^- conformation, the oxygen of this 2′-hydroxyl group comes near to H-5′ of the -pN residue by about 2.5 Å when the sugar pucker is ^3E for both the nucleotidyl units. The data in Table VIII indicate that in all the dimers examined the H-5′ of the -pN residue undergoes substantial deshielding. This suggests that all dimers show significant population of g^-g^- conformer. In addition, the data indicate that in ϵApϵA and ApA the H-5′ is deshielded almost to the same extent which clearly suggests that both nucleic acid systems have comparably the same population of g^-g^- conformer. The presence of g^-g^- stacked arrays will also be reflected in the dimerization shift data for the base protons. It is important to emphasize that only in the g^-g^- stacked array

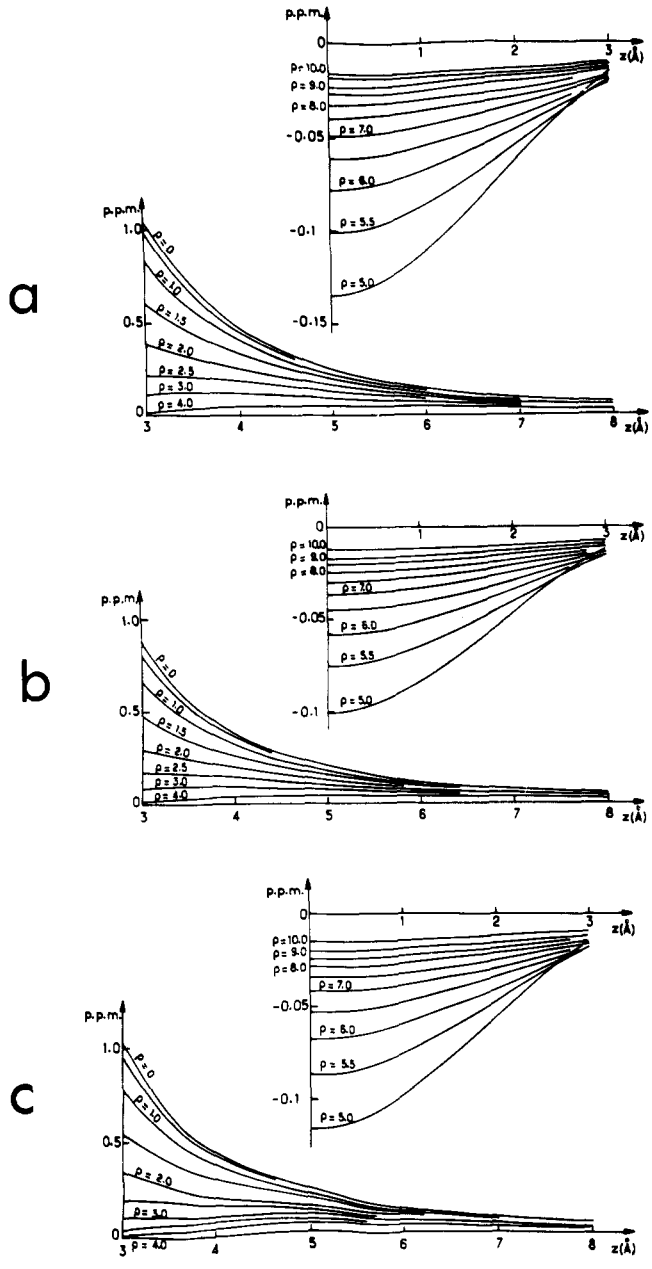

FIGURE 10: Intermolecular isoshielding curves ($\Delta\delta$) of the three rings of 1-N^6-ethenoadenosine as a function of $|z|$, the vertical distance from the base plane: (a) ρ_6 in angstroms is the radius from the center of the six membered ring; (b) ρ_5 in angstroms is the radius from the center of the five-membered ring (N-7-N-9); (c) ρ_5' in angstroms is the radius from the center of the five-membered ring (N-1-N-6).

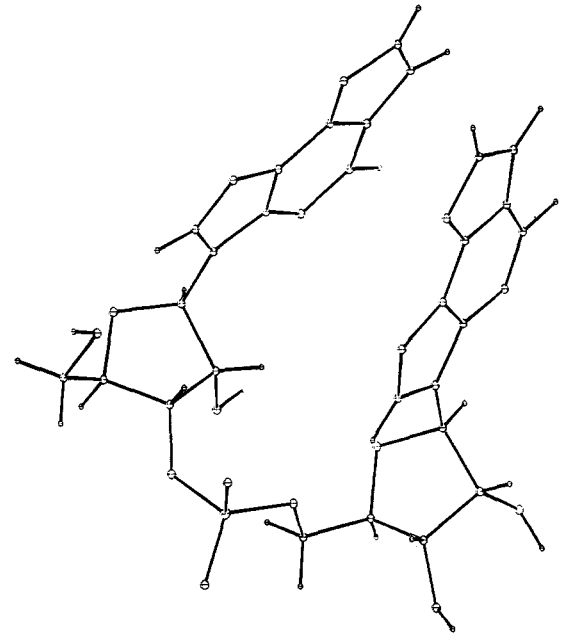

FIGURE 11: A perspective of ϵApϵA in the g^-g^- conformation ($\omega' = 285°$, $\omega = 295°$, $\chi_1 = 25°$, $\chi_2 = 40°$). The rest of the torsion angles are those in Figure 4.

the base overlap and base separation permit the base protons to experience ring-current upfield shifts, i.e., the observed upfield shifts of the base protons essentially reflect the presence of g^-g^- stacks. In the g^+g^+ loop stack, the base separation is too large to result in any ring-current shifts for the base protons. In order to determine the molecular topology of ϵApϵA, we have made a search in the g^-g^- conformation space which will account for the observed dimerization shifts. The methodology employed is described in detail elsewhere (Dhingra and Sarma, 1978a,b; Cheng and Sarma, 1977a). Using this methodology and the ring-current profiles in Figure 10, as well as using all the previous reported torsion angles except for χ_1, χ_2, ω', and ω, we have arrived at the preferred g^-g^- conformation. In this conformation, $\omega' = 285°$, $\omega = 295°$, $\chi_1 = 25°$, and $\chi_2 = 40°$; the perspective of this conformation is shown in Figure 11 and it is very similar to that derived for ApA (Dhingra and Sarma, 1978a). The derived cylindrical coordinates, the projected shieldings, and the observed shieldings in parts per million for the base protons of the ϵAp residue in this conformation are given in Table IX. The data indicate that there is an agreement between the projected and observed shifts, except for H-8. In order to account for the shift of H-8 proton, we have made an intensive search in the g^-g^- conformation and found that when ω' is changed to 300°, ω to 290°, and χ_2 to 45°, the projections for H-8 proton agreed with the observed value, but the remaining base protons experience only a very small shielding effect (Table IX). Similarly, for the -pϵA residue, no single conformation could explain the observed dimerization shifts for the base protons. However, a blend of conformers, in which the various torsion angles (ω', ω, χ_1, and χ_2) are ±5° off from the conformation arrived at from the dimerization shift data for the ϵAp- residue, could reasonably explain the observed dimerization shifts for the base protons (Table X).

Hence, the observed dimerization data for the base protons of both the residues in ϵApϵA can be explained based on an average conformation in the g^-g^- domain in which ω' ranges from 285° to 300° and $\omega \simeq 295 \pm 5°$, $\chi_1 = 25° \pm 5$, and $\chi_2 \simeq 45° \pm 5°$. It is very difficult to determine whether a local domain (285° to 300°) for ω' and fluctuations in other torsion angles exists in the g^-g^- conformation space for ApA. This is simply because in ApA the bases are not large enough and the protons in the bases are not sufficiently separated in space to monitor minor fluctuations in the geometry.

Even though ApA and ϵApϵA have comparable populations of g^-g^- conformer, a clear difference exists in the population distribution of loop stack and skewed and extended arrays. We have shown before that the skewed array g^+t will manifest in the substantial shielding of H-5′ and H-5″ of the Np- residue (Table VI). The data in Table V show that these protons have undergone a shielding of 0.192 and 0.131 ppm, respectively, in ϵApϵA, whereas the corresponding values in ApA are 0.009 and 0.024 ppm. This observed difference is not due to differences in the ring-current fields between adenine and ϵA be-

TABLE IX: Cylindrical Coordinates z, ρ_6, ρ_5, ρ_5'[a] in Angstroms and Projected Shieldings in Parts per Million for the Base Protons of the ϵAp- Residue in the g⁻g⁻ Conformation Space.[a]

proton	cylindrical coordinates				projected shieldings				obsd shielding,
	z	ρ_6	ρ_5	ρ_5'[a]	δ_6	δ_5	δ_5'	δ_{total}	δ_{obsd}
				conformation: $\omega' = 285°$; $\rho_1 = 25°$; $\omega = 295°$; $\chi_2 = 40°$					
H-2	4.7	1.8	3.1	4.1	0.28	0.06	0.05	0.39	0.409
H-8	4.8	5.1	3.2	5.9	0.00	0.06	0.00	0.06	0.324
H-10	4.5	2.6	4.9	2.3	0.20	0.00	0.25	0.45	0.449
H-11	4.4	3.8	4.7	1.2	0.06	0.00	0.43	0.49	0.534
				conformation: $\omega' = 300°$; $\chi_1 = 25°$; $\omega = 290°$; $\chi_2 = 45°$					
H-2	4.0	3.5	4.1	5.5	0.06	0.02	0.00	0.08	
H-8	4.6	3.7	2.2	4.0	0.05	0.20	0.05	0.30	
H-10	3.2	3.6	5.4	4.6	0.05	0.00	0.00	0.05	
H-11	3.0	3.6	5.7	3.1	0.05	0.00	0.10	0.15	

[a] $\rho_5' = \rho_5(N_1 - N_6)$.

TABLE X: Cylindrical Coordinates z, ρ_6, ρ_5, ρ_5' in Angstroms and Projected Shieldings in Parts per Million for the Base Protons of the -pϵA Residue in the g⁻g⁻ Conformation Space.

proton	cylindrical coordinates				projected shieldings				obsd shieldings,
	z	ρ_6	ρ_5	ρ_5'	δ_6	δ_5	δ_5'	δ_{total}	δ_{obsd}
				conformation: $\omega' = 285°$; $\chi_1 = 25°$; $\omega = 295°$; $\chi_2 = 40°$					
H-2	4.6	3.5	5.6	2.8	0.06	0.00	0.13	0.19	0.338
H-8	4.9	3.0	1.9	5.0	0.08	0.20	0.00	0.28	0.324
H-10	4.4	4.5	5.9	2.4	0.00	0.00	0.23	0.23	0.228
H-11	4.4	4.8	5.2	2.9	0.00	0.00	0.12	0.12	0.231
				conformation: $\omega' = 285°$; $\chi_1 = 25°$; $\omega = 290°$; $\chi_2 = 50°$					
H-2	3.4	3.4	5.5	2.9	0.06	0.00	0.13	0.18	
H-8	5.1	2.9	1.9	4.9	0.10	0.15	0.00	0.25	
H-10	3.0	4.3	5.8	2.2	0.00	0.00	0.35	0.35	
H-11	3.3	4.6	5.1	2.7	0.00	0.00	0.25	0.25	
				conformation: $\omega' = 300°$; $\chi_1 = 25°$; $\omega = 290°$; $\chi_2 = 45°$					
H-2	3.3	3.3	4.9	1.4	0.06	0.00	0.40	0.46	
H-8	4.8	3.0	1.4	4.8	0.10	0.25	0.00	0.35	
H-10	3.0	5.2	5.8	3.3	0.00	0.00	0.08	0.08	
H-11	3.3	6.0	5.6	4.7	0.00	0.00	0.02	0.02	

TABLE XI: Cylindrical Coordinates z, ρ_6, ρ_5, ρ_5' in Angstroms and Projected Shieldings in Parts per Million for H-5′ and H-5″ of the ϵAp- Residue in Various Conformations.

conformation	proton	cylindrical coordinates				projected shielding			
		z	ρ_6	ρ_5	ρ_5'[a]	δ_6	δ_5	δ_5'[a]	δ_{total}
g⁺g⁺ ($\omega' = 80°$; $\omega = 80°$)	H-5′	6.4	4.8	3.0	7.0	0.02	0.10	0.00	0.12
	H-5″	4.9	5.3	3.5	7.4	0.0	0.08	0.00	0.08
g⁺t ($\omega' = 110°$; $\omega = 215°$)	H-5′	4.1	2.8	1.2	3.7	0.18	0.35	0.03	0.56
	H-5″	3.1	3.5	1.5	4.8	0.06	0.45	0.00	0.51
tg⁺ ($\omega' = 180°$; $\omega = 80°$)	H-5′	7.2	5.7	3.8	6.5	0.03	0.00	0.00	0.03
	H-5″	5.6	5.4	3.4	6.2	0.05	0.00	0.00	0.05

[a] $\rho_5' = \rho_5(N_1 - N_6)$.

cause the extra five-membered ring (N-1–N-6) has very little shielding effect on H-5′ and H-5″ of the Np- residue in the g⁺t conformation. This is evident from an examination of the cylindrical coordinates and the projected shieldings in Table XI. This means that in ϵApϵA there is a significantly larger fraction of the g⁺t conformer compared to ApA. A perspective of ApϵA in the g⁺t conformer is shown in Figure 12. The lack of significant shielding of H-5′ and H-5″ of the Ap- residue of ApA (Table V) enables us to conclude that no significant amount of g⁺t conformer is present in ApA.

A comparison of the dimerization shifts for H-5′ (Table VIII) of ApϵA and ApA indicates that introduction of ϵA for the base of the -pN residue causes a decrease in the population of g⁻g⁻ stack, while a comparison of the dimerization shifts of H-5′ and H-5″ protons of Np- residues in ApϵA and ApA (Table V) clearly indicates that introduction of ϵA causes a substantial increase in the population of the g⁺t conformer; i.e., in going from ApA to the ApϵA, the g⁻g⁻ population decreases while that of g⁺t increases. A comparison of the dimerization data for GpA and GpϵA indicates that the introduction of ϵA in the -pN residue destabilizes the g⁻g⁻ conformer and increases the population of the g⁺t array. Similarly, the data for ϵApG and ApG (Tables V and VIII) indicate that they have comparable g⁻g⁻ populations, but in the ϵA ana-

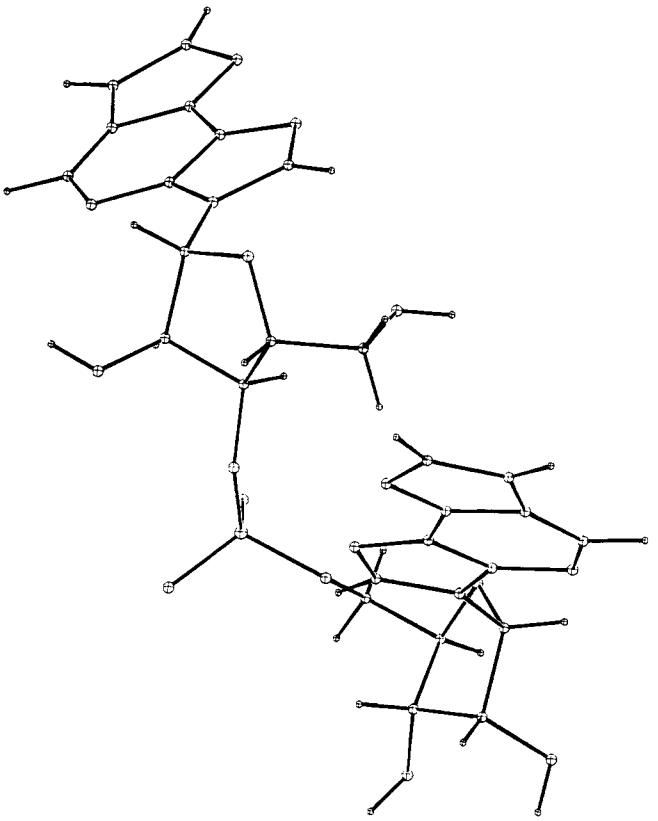

FIGURE 12: A perspective of ϵApϵA in the g$^+$t conformation (ω' = 110°, ω = 215°, χ_2 = 50°). The rest of the torsion angles are those in Figure 5.

logue the population of the g$^+$t conformer increases. Comparison of the matched pair ϵApG and GpϵA gives insight in regards to the ability of ϵA to disturb the conformational equilibrium, depending whether it is located either at the 3′ or 5′ end. When ϵA is moved from the 3′ to the 5′ end, the g$^-$g$^-$ population increases (Table VIII) and the g$^+$t population decreases (Table V). In general, the comparison of the ϵA-containing dimers with the corresponding parent dimers in the PUPU system clearly suggests that the introduction of ϵA either at the 3′ or 5′ end causes a significant increase in the population of skewed g$^+$t arrays, the increase being larger when the replacement occurs at the 3′ end.

In the case of mixed dimers, for example, in going from UpA to UpϵA, the H-5′ and H-5″ protons of the Np- residue (Table V) undergo substantial shielding (δ H-5′ = 0.44 ppm, δ H-5″ = 0.24 ppm), clearly indicating a significant increase in the population of the g$^+$t array. Such large upfield shifts for the H-5′ and H-5″ protons of the Np- residue have never been observed before. The data, for the various PYPU and PUPY dimers examined, indicate that the introduction of ϵA either at the 3′ or 5′ end causes an increase in the g$^-$g$^-$ population. In addition, as stated before, in these systems the introduction of ϵA at the 3′ end causes a substantial increase in the g$^+$t population. NMR methodology does not enable us to determine whether ϵA at the 5′ end in PUPY dimers as in ϵApU will have the same effect because of the lack of a ring current from the pyrimidine moiety (Lee et al., 1976).

Relevance to tRNA Conformation. The present study, as well as the large number of theoretical and NMR studies (references given earlier), has enabled us to conclude that all the ribodinucleoside monophosphates exist in aqueous solution as an equilibrium blend of stacked (g$^-$g$^-$, g$^+$g$^+$), skewed (g$^+$t), and extended arrays, and no methodology exists to compute accurately the fraction of each one of them. Introduction of ϵA either at the 3′ or 5′ end causes a shift in the equilibrium, generally increasing the population of skewed (g$^+$t) arrays. Examination of the nucleotide sequence of tRNA^{Phe} (Brennan and Sunderalingam, 1976; Stout et al., 1976) indicates that the segment comprising residues 36 and 37 may be approximated to ApϵA and GpϵA. The data discussed in this paper clearly show that the introduction of ϵA in the parent dimers ApA and GpA causes a decrease in the g$^-$g$^-$ population with the concomitant increase in the g$^+$t skewed arrays. This observation suggests that at least in aqueous solution one of the probable roles of the Y base in tRNA may be to introduce a backbone conformational change.

It is pertinent to point out that in all of these calculations for the projected shieldings only the firmly established ring-current effects of the bases are taken into consideration. There are other through space magnetic (diamagnetic susceptibility anisotropy) and electric-field (polarization) effects that may contribute to the observed values of chemical shifts in nucleic acids. The local diamagnetic anisotropy effect of the base is, at most, 0.2–0.3 ppm at intermolecular distances (Giessner-Prettre and Pullman, 1976), and this type of contribution due to the ribose part of the molecule will have some importance only for the regions of the space close to the oxygen atoms. The electric field or polarization effect, which is very sensitive to the orientation of the C–H bond with respect to the direction of the electric field created by the polarizing groups at the proton studied, will be of some importance only for a few protons of the dimers. The ring-current effects are the largest single effect, and the consideration of these effects alone should give agreement at the level of 0.1 to 0.2 ppm.

Acknowledgment

We thank Professor Tinoco, Jr., and Dr. C. H. Lee for excellent cooperation and providing us the microfilm data. We also thank the University Computer Center, particularly Mr. J. Quinn, for assistance in the course of this work.

References

Brennen, T., and Sundaralingam, M. (1976), *Nucleic Acid Res. 3,* 3235.

Cheng, D. M., and Sarma, R. H. (1977a), *J. Am. Chem. Soc. 99,* 73333.

Cheng, D. M., and Sarma, R. H. (1977b), *Biopolymers 16,* 1687.

Dhingra, M. M., and Sarma, R. H. (1978a), *Nature (London) 272,* 798.

Dhingra, M. M., and Sarma, R. H. (1978b), Proceedings International Symposium on Biomolecular Structure, Conformation, Function and Evolution, Srinivasan, R., Ed., Elmsford, N.Y., and Oxford, Pergamon Press (in press).

Ezra, F. S., Lee, C. H., Kondo, N. S. Danyluk, S. S., and Sarma, R. H. (1977), *Biochemistry 16,* 1977.

Giessner-Prettre, C., and Pullman, B. (1965), *C. R. Hebd. Seances Acad. Sci. 261,* 2521.

Giessner-Prettre, C., and Pullman, B. (1969) *C. R. Hebd. Seances Acad. Sci., Ser. D 268,* 1115.

Giessner-Prettre, C., and Pullman, B. (1970), *J. Theor. Biol. 27,* 87.

Giessner-Prettre, C., and Pullman, B. (1976), *Biochem. Biophys. Res. Commun. 70,* 578.

Giessner-Prettre, C., and Pullman, B. (1977), *J. Theor. Biol. 65,* 189.

Giessner-Prettre, C., and Pullman B. (1978), *Jerusalem Symp. Quantum Chem. Biochem. 11* (in press).

Giessner-Prettre C., Pullman, B., Borer, P. N., Kan, L. S., and

Ts'o, P. O. P. (1976), *Biopolymers 15,* 2277.
Govil, G. (1976), *Biopolymers 15,* 2303.
Hingerty, B., Subramanian, E., Stellman, S. D., Broyde, S. B., Sato, T., and Langridge, R. (1975), *Biopolymers 14,* 227.
Johnson, E. D., and Bovey F. A. (1958), *J. Chem. Phys. 29,* 1012.
Kim, S. H., Berman, H. M., Seeman, N. C., and Newton, M. D. (1973), *Acta Crystallogr., Sect. B 29,* 703.
Lee, C. H., and Tinoco, I., Jr. (1977), *Biochemistry 16,* 5403.
Lee, C. H., Ezra, F. S., Kondo, N. S., Sarma, R. H., and Danyluk, S. S. (1976), *Biochemistry 15,* 3627.
Perahia, D., Pullman, B., and Saran, A. (1974), *Biochim. Biophys. Acta 340,* 299.
Remin, M., and Shugar, D. (1972), *Biochem. Biophys. Res. Commun. 48,* 636.
Rubin, J., Brennan, T., and Sundaralingam, M. (1972), *Biochemistry 11,* 3112.
Seeman, N. C., Rosenberg, J. M., Suddath, F. L., Kim, J. J. P., and Rich, A. (1976), *J. Mol. Biol. 104,* 109.
Son, T. D., and Guschlbauer, W. (1975), *Nucleic Acids Res. 2,* 873.
Stout, C. D., Mizuno, H., Rubin, J., Brennan, T., Rao, S. T., and Sundaralingam, M. (1976), *Nucleic Acids Res. 3,* 1111.
Waugh, J. S., and Fessenden, R. W. (1957), *J. Am. Chem. Soc. 79,* 846.

Resonance Raman Studies of Hepatic Microsomal Cytochromes P-450: Evidence for Strong π Basicity of the Fifth Ligand in the Reduced and Carbonyl Complex Forms†

Yukihiro Ozaki, Teizo Kitagawa,* Yoshimasa Kyogoku, Yoshio Imai, Chikako Hashimoto-Yutsudo, and Ryo Sato

ABSTRACT: Resonance Raman spectra have been measured for cytochromes P-450 purified from liver microsomes of phenobarbital-treated rabbits (PB P-450 and PB P-448) and of 3-methylcholanthrene-treated rabbits (MC P-448). In the reduced state, all three cytochromes P-450 exhibit Raman spectra of ferrous high-spin type but show the so-called "oxidation state marker" (band IV) at unusually low frequencies, indicating extensive delocalization of electrons from the iron d_π orbital to the porphyrin $\Pi^*(e_g)$ orbital and, consequently, the strong π basicity of the fifth ligand of the heme iron. The reduced CO complexes of the cytochromes P-450 also exhibit band IV at markedly lower frequencies than CO complexes of hemoglobin and myoglobin. These anomalies observed for the reduced form and CO complex disappear upon conversion of the cytochromes to the catalytically inactive form called cytochrome P-420. Oxidized PB P-450 shows a Raman spectrum which is characteristic of typical ferric low-spin heme compounds, whereas those of PB P-448 and MC P-448 are of the ferric high-spin type. PB P-450 is also clearly distinguishable from the two P-448 preparations in the reduced state. The reduced form of cytochrome P-420, produced by laser illumination, exhibits two sets of Raman lines and, therefore, seems to be a mixture of both high- and low-spin species.

Cytochrome P-450 (P-450)[1] is a generic name for a family of protoheme-containing proteins that are widely distributed in nature and catalyze a variety of monooxygenation (hydroxylation) reactions of metabolic importance. The reduced CO complex of this class of hemoproteins exhibits the Soret absorption band at about 450 nm, a wavelength which is approximately 30 nm longer than that observable for usual ferrous protoheme–CO complexes (Sato et al., 1973). This and other spectral anomalies of P-450 disappear when it is converted into the catalytically inactive form called cytochrome P-420 (P-420) by various treatments (Sato et al., 1973). Currently, extensive efforts are being made to elucidate the structural basis of the spectral anomalies of P-450 by both physicochemical and coordination chemical approaches.

It has been shown that synthetic protohemin complexes having a thiolate anion (RS^-) and an arbitrary nitrogenous base as axial ligands to the heme iron display electron paramagnetic resonance (EPR) spectra that are closely similar to that exhibited by P-450 in the ferric low-spin state (Collman et al., 1975; Koch et al., 1975; Tang et al., 1976; Ogoshi et al., 1975). Model experiments have also provided evidence that the heme in the substrate complex of oxidized P-450 is in the pentacoordinated high-spin state possessing a thiolate anion as the fifth ligand (Collman et al., 1975; Tang et al., 1976). These conclusions are being supported by Mössbauer (Koch et al., 1975) and magnetic circular dichroism (MCD) studies (Dawson et al., 1976). Nuclear magnetic resonance (NMR) (Keller et al., 1972) and Mössbauer spectra (Sharrock et al., 1973) of the substrate complex of reduced P-450 have suggested that its heme iron is in the ferrous high-spin state. It has further been reported that synthetic ferrous protoheme complexes having a thiolate anion, but not a nitrogenous base, as a ligand trans to CO exhibit the unusual Soret absorption band characteristic of the CO complex of reduced P-450 (Stern and

† From the Institute for Protein Research, Osaka University, Suita Osaka 565, Japan. *Received May 17, 1978.*

[1] Abbreviation used are: P-450, cytochrome P-450; $P\text{-}450_{cam}$, cytochrome P-450 from camphor-grown *Pseudomonas putida*; P-420, cytochrome P-420; Hb, hemoglobin; Mb, myoglobin; EPR, electron paramagnetic resonance; NMR, nuclear magnetic resonance; MCD, magnetic circular dichroism; CM, carboxymethyl.

0006-2960/78/0417-5826$01.00/0 © 1978 American Chemical Society